Atomic Spectroscopy

Article

In Situ Analysis of Low-Li-Be Samples by Secondary Ion Mass Spectrometry

Qing Yang,[a] Zexian Cui,[a] Xiao-Ping Xia,[b,*] Chun-Kit Lai,[c] Wan-Feng Zhang,[a] and Yan-Qiang Zhang[a]

[a] State Key Laboratory of Isotope Geochemistry, Guangzhou Institute of Geochemistry, Chinese Academy of Sciences, Guangzhou 510640, P. R. China

[b] Hubei Key Laboratory of Petroleum Geochemistry and Environment, College of Resources and Environment, Yangtze University, Wuhan 430100, P. R. China

[c] Global Project Generation and Targeting, Fortescue Metals Group Ltd., East Perth, Western Australia 6004, Australia

Received: *February 28, 2024;* ***Revised:*** *March 21, 2024;* ***Accepted:*** *March 25, 2024;* ***Available online:*** *March 27, 2024.*

DOI: 10.46770/AS.2024.037

ABSTRACT: Lithium and beryllium are strategic key metals, which are indispensable in emerging information technology and green energy industries. They are also powerful tracers in a wide range of geological processes, notably those related to deep-earth elemental cycling and ore deposition. Secondary ion mass spectrometry (SIMS) analysis has the advantages of in situ, high spatial resolution and almost non-destruction. Here, we present a modified SIMS procedure to simultaneously measure the Li-Be contents in eight well characterized Li-Be-poor glass samples (Li = 3−43 ppm, Be = 0.034−46 ppm) and one new synthetic glass with purity (considered as Li and Be free) to evaluate the analytical precision, accuracy and limit of detection (LOD). For lithium, the internal precision is better than 0.42% (1SE), and the spot-to-spot reproducibility is mostly better than 2.71% (RSD). For beryllium, the internal precision is better than 0.93% (1SE), and the spot-to-spot reproducibility is better than 4.68% (RSD). For the Li and Be contents, the difference between the calibrated SIMS elemental contents and the recommended value is generally below 5.1% and 7.9%, respectively. The LOD is ~0.04 ppb for Li and ~0.01 ppb for Be. All these demonstrate the improved performance of this analytical technique and its reliability for measurement of low-Li-Be samples. The findings contribute to our understanding of the Li-Be distribution and behavior in geological materials, and provide implications to mineral exploration and environmental studies.

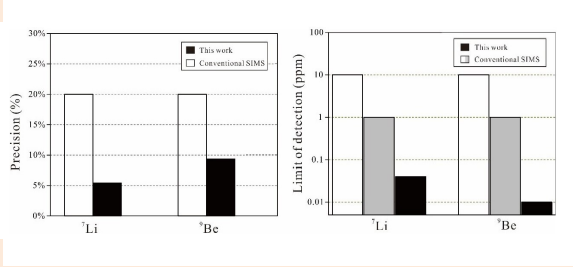

INTRODUCTION

Strategic key metals, including lithium (Li) and beryllium (Be), commonly have high supply risk and diverse applications in emerging industries, such as aerospace, green energy and information technology.[1-6] Lithium is the metal with the lowest atomic number, and the first member of the alkali metal group. It is an excellent conductor of electricity and heat,[7, 8] and is widely used for power batteries and special engineering plastics.[9, 10] Beryllium has the advantages of metal fatigue and corrosion resistance, insulation, non-magnetic, and light, with a wide range of applications in aerospace and medical industries.[11] Lithium and beryllium are also important tracers in modern petrogenesis, especially in metallogenic studies.[12] There are various Li and Be ore deposits, including those hosted by granite-pegmatite, volcanic-sedimentary rocks, and salar.[7, 11, 13-16] Their elemental budgets and cycling across the Earth's different spheres and metallogenic mechanisms are important geoscientific research topics.[9, 11, 13, 16-19]

Lithium concentration can be measured by bulk-sample analysis, spectral analysis, chromatography, electron probe microanalysis (EPMA), laser ablation inductively coupled mass spectrometry (LA-ICP-MS), and secondary ion mass spectrometry (SIMS), depending on the sample and the level of precision required.[8, 20-36] In situ micro analyses including EPMA, LA-ICPMS and SIMS, are required for most earth science studies due the highly complex compositional variation on small geological samples. Among them, EPMA measurements of Li contents have always serious signal interference and relatively high detection limits (80 ppm).[37] Evaluation works on this Li

analysis technique are rare.[34, 37] LA-ICP-MS has good analytical precision (1.4 ppm, RSD = 0.2%) and relatively low detection limits (0.056 ppm),[27] but the limit of detection (LOD) value is still insufficient to accurately characterize Li distribution in geological materials, and hampered a better understanding of its role in geological processes and resource exploration. It also suffers low spatial resolution (>32 μm) and large sample consumption.[12, 27, 31, 32] As for Be analysis, the used in situ micro analyses techniques include EPMA, LA-ICP-MS and SIMS.[6, 12, 27, 29, 38-43] EPMA can be problematic because: a) Be is a very light element with long wavelength and low energy; b) The characteristic X-ray intensity and peak-to-background ratio of Be element are relatively low; c) The heavy elements (*i.e.*, Si, P) -induced X-ray lines have apparent interference in Be Kα line; d) There is drift of Be characteristic peak.[6, 44, 45] Despite these short falls and inherent high detection limit (>250 ppm for Be), EPMA has the advantages of being in situ, non-destructive, and has high spatial resolution (suitable for fine-grained minerals).[6, 43] Compared with EPMA, LA-ICP-MS has a lower detection limit (ppb-scale), but again its spatial resolution is lower. Thus, LA-ICP-MS is more suitable for analyzing coarser-grained minerals with higher internal homogeneity.[12, 29] For both Li and Be element/isotope analyses, SIMS analysis has the advantages of almost non-destruction, high-resolution (μm-/nm-scale), high accuracy, and low detection limit.[8, 36, 39, 40, 42] Ottolini *et al.* proposed a SIMS analytical procedure to measure lithium and beryllium contents with low mass resolution (MRP, 10%) about 600. "Energy-filtered" analyses were used in order to discriminate Al^{3+} interference from Be^{+} ions. This method has a low ionization yield of target ions and a low precision (20%).[46] Moreover, the counting times of this method were relatively long. It is 100 s/cycle for lithium and beryllium, and 10 s/cycle for silicon, total 10 cycles were used which were too long for precious SIMS analysis time.[46] Cabato *et al.* improved the MRP to about 1000, but the problems of low ionization yield and low precision still remain.[47]

In this study, by improving the mass resolution and the ionization efficiency of the secondary ions, we shorten the counting time, improve the efficiency of the instrument, and establish an accurate and precise measurement method of low content Li-Be elements. The accuracy, precision and LOD of Li-Be were evaluated by analyzing nine glasses with trace Li-Be contents.

EXPERIMENTAL

Sample descriptions and preparation. In this study, we analyzed eight well characterized glass standards and one new synthetic glass. The eight well characterized glass standards include five basaltic glass of BCR-2G (Li = 9 ± 1 ppm, Be = 2.3 ± 0.4 ppm, 1SD),[29, 48-54] BHVO-2G (Li = 4.4 ± 0.8 ppm, Be = 1.3 ± 0.2 ppm),[50-54] BIR-1G (Li = 3.0 ± 0.7 ppm, Be = 0.10 ± 0.01 ppm),[52, 53] GSD-1G (Li = 43 ± 6 ppm, Be = 46 ± 5 ppm),[51-54] and KL2-G (Li = 5.10 ± 0.25 ppm, Be = 0.88 ± 0.17 ppm),[12, 29, 41, 52, 54, 55] one quartz-diorite glass T1-G (Li = 19.90 ± 0.45 ppm, Be = 2.00 ± 0.36 ppm),[12, 29, 41, 52, 54, 55] one komatiite glass GOR128-G (Li =10.40 ± 0.85 ppm, Be = 0.034 ± 0.003 ppm),[12, 29, 41, 52, 54, 55] and one dacite glass StHs6/80-G (Li = 20.7± 1.2 ppm, Be = 1.2 ± 0.05 ppm) (Table 1).[29, 41, 52, 54] Chemical compositions for these standards are mostly from the open-source GeoRem database (http://georem.mpch-mainz.gwdg.de/), except for the Be content of BIR-1G,[52, 54] which is absent in the database. Detailed sample descriptions have been extensively reported,[12, 27, 29, 41, 49-55] and are not repeated here. The new synthetic glass, HPFS® 7979 (hereafter abbreviated as 7979), used in this study was a silicate glass purchased from the dealer Shanghai Ruitai Optoelectronics Technology Co. Ltd.. It is a high-purity non-crystalline silica glass with excellent optical qualities produced by the Corning Co. Ltd. (Table 1). This highly pure glass is taken as a Li-Be free sample for estimation of LOD. All analyzed glass samples were large fragments of 0.3–1.5 mm in diameter, which were embedded into a standard epoxy SIMS mount and polished to a flat and even surface. Thorough cleaning before analysis involved repeated ultrasonic cleaning with high-purity ethanol and deionized water.

Table 1. Sample information

Standards	Li (ppm)	1SD	Be (ppm)	1SD	SiO_2 (%)
BCR-2G	9	1	2.3	0.4	54.4
BHVO-2G	4.4	0.8	1.3	0.2	49.3
BIR-1G	3	0.7	0.1	0.01	47.5
GOR128-G	10.4	0.85	0.034	0.003	46.1
GSD-1G	43	6	46	5	53.2
KL2-G	5.1	0.25	0.88	0.17	50.3
StHs6/80-G	20.7	1.2	1.2	0.05	63.7
T1-G	19.9	0.45	2	0.3	58.6
7979	2.25E-04[a]	0.14E-04[a]	1.59E-05[a]	0.45E-05[a]	100

Note: Data are mostly from GeoRem (http://georem.mpch-mainz.gwdg.de/), except for the BIR-1G Be content [52, 54] and the data for 7979 are from this study SIMS value.

Instrumentation and operating conditions. The Li-Be contents were measured with a CAMECA IMS 1280-HR SIMS instrument at the State Key Laboratory of Isotope Geochemistry (SKLaBIG), Guangzhou Institute of Geochemistry, Chinese Academy of Sciences (GIGCAS). A primary O^{-} beam, accelerated to 13 kV with a current intensity of 11-19 nA, was used. Positively charged secondary ions were accelerated at +10 kV potential. Gaussian illumination mode was adopted to produce an elliptical 15 μm × 10 μm spot, and a 15 μm × 15 μm raster was applied to ensure a flat-bottomed pit. The entrance slit and field aperture were set to 380 μm and 5000 μm, respectively. Combined with an energy slit of 50 eV bandwidth, a mass resolution power of 2000 (50% peak width) was achieved to avoid interference from $^{27}Al^{3+}$.[12, 46] Each measurement typically comprises a 90 s pre-analysis sputtering, which used a 30 μm × 30 μm raster to clean the sample surface and

Table 2. SIMS measured value of $^{7}Li/^{28}Si$ and $^{9}Be/^{28}Si$

Standard materials	Sample Number	Measured $^{7}Li/^{28}Si$	RSD (%)	Rejected	Measured $^{9}Be/^{28}Si$	RSD (%)	Rejected
BCR-2G	15	8.90E-04	0.99	0	3.11E-05	0.44	0
BHVO-2G	15	5.16E-04	1.73	0	1.64E-05	0.50	0
BIR-1G	15	3.70E-04	1.48	0	1.48E-06	0.77	0
GOR128-G	14	1.36E-03	2.71	1	7.17E-07	4.68	1
GSD-1G	15	4.39E-03	1.10	0	6.12E-04	0.46	0
KL2-G	15	6.80E-04	0.83	0	1.35E-05	0.47	1
StHs6/80-G	15	1.71E-03	0.94	0	1.56E-05	0.75	0
T1-G	14	1.88E-03	0.79	0	2.76E-05	0.49	0
7979	6	1.23E-08	6.29	0	1.13E-10	28.43	0

Table 3. Calibrated Li and Be contents

Sample	Li content (ppm)	[a]Bias (%)	Be content (ppm)	[b]Bias (%)
BCR-2G	8.86	-0.39	2.39	0.92
BHVO-2G	4.65	1.40	1.14	-3.26
BIR-1G	3.22	1.74	0.10	-0.15
GOR128-G	11.46	2.43	0.05	7.84
GSD-1G	42.75	-0.15	46.00	0.00
KL2-G	6.26	5.09	0.96	2.19
StHs6/80-G	19.97	-0.90	1.40	3.92
T1-G	20.17	0.33	2.29	3.35

[a] Bias is calculated as [(Li calibrated – recommended value)/(Li calibrated + recommended value)]/2*100; [b] Bias is calculated as [(Be calibrated – recommended value)/(Be calibrated + recommended value)]/2*100; Negative bias means that calibrated SIMS value is smaller than the recommended value.

to attain a stable count rate on detectors. A peak jump model sequentially measures the mass of ^{7}Li, ^{9}Be, and ^{28}Si, and 20 cycles were collected, making a single analysis to last 11 minutes. The Faraday cup with a 10^{10} Ω resistor (mono-collector system) was used to detect ^{28}Si, while the electron multiplier (EM) (mono-collector system) was used to detect ^{7}Li and ^{9}Be. Before each analysis session, the Faraday cup and the electron multiplier high voltage were calibrated to ensure their consistent yielding. The waiting time and counting time for ^{7}Li, ^{9}Be, and ^{28}Si in each mass scan cycle are 3, 1.5 and 3 seconds and 4, 8 and 2 seconds, respectively. Peak centering was performed before each analysis by centering the peak of ^{28}Si, which was also used as the internal reference signal. The glass Li-Be contents were calculated from the measured $^{7}Li/^{28}Si*SiO_2$ and $^{9}Be/^{28}Si*SiO_2$ intensity ratios. The SiO_2 content (in wt%), used as the inner reference for SIMS quantification, was derived from previous reports.[12, 29, 41, 48-55] The use of ion intensity ratios with respect to a matrix reference element (generally Si) is necessary because the absolute ion intensity for each element is a very sensitive function of both the local sample surface properties and the operating conditions.

RESULTS AND DISCUSSION

The analytical precision discussed here encompasses both internal (intra-spot, SE) and external (reproducibility) precision of spot-to-spot results (SD/RSD). The internal precision was calculated by the standard error of the analytical results for the different cycles in a single-spot analysis. One SIMS measurement session was conducted to check the analytical precision, accuracy, and LOD, with the results listed in Supporting information Tables S1 and S2 and summarized in Tables 2 and 3.

Analytical precision. The internal precision correlates strongly with counting statistics, which are directly related to the Li-Be

Fig. 1 Reproducibility of the intensity ratios of lithium element to the internal standard element silicon in eight glasses. Error bar denotes 2SE (standard error), whilst he central solid lines denote the external reproducibility (2SD).

Fig. 2 Reproducibility of the intensity ratios of beryllium element to the internal standard element silicon in eight glasses. Error bar denotes 2SE (standard error), whilst he central solid lines denote the external reproducibility (2SD).

contents, the total counting time, and the primary ion intensity. Potential influence of these factors on the internal precision has already been discussed in previous works,[56-59] and is thus not repeated here. For lithium, the internal precision (1SE) of a single analysis for each sample range from 0.14% (StHs6/80-G) to 0.42% (GSD-1G) (Table S1). For beryllium, they range from 0.03% (GSD-1G) to 0.93% (GOR128-G) (Table S1).

The external precision depends on the material homogeneity and instrumental stability, which are influenced by environmental variation and drift of the electron multiplier. Previous studies have shown that high external precision in SIMS isotope analyses requires high-quality sample preparation (*e.g.*, flat surface) and a confined analysis area.[60] Figs 1 and 2 show the reproducibility of the intensity ratios of lithium and beryllium to the internal standard element silicon in eight glasses, respectively. Error bars are ±2SE (standard error), whilst the central solid lines denote the external reproducibility (2SD). The external precision of our Li analysis is 0.79 to 2.71% (RSD), among which that of sample T1-G is the best (0.79%, Li = 19.9 ppm), and that of the lowest-Li (3 ppm) sample BIR-G is 1.48%, which is much better than the precision of GOR128-G (2.71%, Li = 10.4 ppm), similar to that of certain previous studies.[8, 12] This indicates that GOR128-G is not very homogenous,[12] which is also evidenced by a discrete point (out of 2SD range) in GOR128-G in Fig. 1. External precision for the Be content ranges from 0.44 to 4.68%, among which the best and worst are BCR-2G (Be = 2.3 ppm) and GOR128-G (Be = 0.034 ppm, the lowest Be sample), respectively. GOR128-G and KL2-G have a discrete point (out of 2SD range, Fig. 2), which may be caused by sample heterogeneity.[12] The lowest external precision (2.71% and 4.68% (1SD), respectively) of lithium and beryllium in this study is much better than the 20% (2SD) reported by Ottolini *et al*.[46] which proves the advantages of the method.

Calibration curve and accuracy. The Li and Be contents were calculated from the measured $^{7}Li/^{28}Si^{*}SiO_2$ and $^{9}Be/^{28}Si^{*}SiO_2$ (Table S2), respectively, and a calibration curve was constructed by analyzing the eight well-characterized glass reference materials. Fig. 3 shows the calibration curves and the reference samples used to construct them. Each data point represents an average SIMS analysis of a single reference sample. The ordinate values for the Li and Be elements, is taken from the previous reports.[12, 29, 41, 48-55] We used the calibration curve ($[Li] = 182.96 \times [^{7}Li/^{28}Si^{*}SiO_2]$; $R^2 = 0.998$, Fig. 3A) and ($[Be] = 1411.83 \times [^{9}Be/^{28}Si^{*}SiO_2]$; $R^2 = 1$, Fig. 3B) to invert the measured $^{7}Li/^{28}Si$ and $^{9}Be/^{28}Si$ intensity ratios into the Li or Be contents, respectively. To assess the analytical accuracy, all the measurements were treated as unknown, and their measured values were calibrated with the calibration curves (Table 3). For the Li content, the difference between the calibrated SIMS elemental contents and the recommended value (summarized in Table 1.[12, 29, 41, 48-55]) is generally < 5.1% (Table 3). The smallest difference (−0.15%) is from GSD-1G, which has the highest content (43 ppm). BIR-1G, the lowest Li sample (3 ppm), has a difference of 1.74%. This is better than the largest difference of 5.09% in KL2-G (5.1 ppm). Therefore, the determination of glass KL2-G may require further examination of its homogeneity. For the Be content, the difference between the calibrated SIMS elemental contents and the recommended value (summarized in Table 1.[12, 29, 41, 48-55]) is generally < 7.9% (Table 3). The smallest difference is also GSD-1G (0.00%), which has the highest content (46 ppm). GOR128-G, the lowest Be sample (0.034 ppm), has the largest difference of 7.84%, which is reasonable (the analytical accuracy of most trace elements is acceptable within 10%) for such a low content.[12]

Limits of detection. LOD strongly depends on the background signal, counting time per element and sensitivity,[12] which can be evaluated based on 3SD of background measurement.[61, 62] It is difficult to find a completely Li- and Be-free sample for background measurement. We took the highly pure 7979 glass as "Li-Be free" sample and calculated its 3SD for LOD evaluation.

Fig. 3 A) Li calibration curve for the eight well known glass samples, B) Be calibration curve for the eight well known glass samples. Lines pass through the origin and the error bar denotes 1SD. Each data point represents an average SIMS analysis of a single reference sample. The ordinate values for the Li and Be elements, is taken from the previous reports.[12, 29, 41, 48-55]

Accordingly, the LOD of lithium yielded ~0.04 ppb, which is significantly better than that of Ottolini *et al.* (10 ppb) and Cabato *et al.* (1 ppb).[46, 47] It is worth noting that the 7979 glass is only nominally Li-Be free, from the raw data (the count rate is about 15 cps, Table S1), there is still a little lithium element in this glass, the LOD of lithium we evaluated will be the upper limit we can find, if there is a suitable sample, the LOD of lithium will theoretically be lower. The LOD of beryllium yielded ~0.01 ppb, which is also significantly better than the previously reported SIMS measurement LOD of ~10 ppb,[46] and 1 ppb.[47] Such a low LOD are satisfactory for most geochemical and crystallo-chemical investigations. The lower LOD in this work may be due to: 1) the high mass resolution (10%MRP = ~ 2000), which is enough to discriminate Al^{3+} interference from Be^{+}, and then the high energy offset was not necessary. This reduces the loss of secondary ions; 2) CAMECA IMS 1280-HR SIMS allows the measurement of lithium and beryllium with two and one order of magnitude higher sensitivity (Li^{+}: ((2-3)×10^3 and Be^{+}: (2-4)×10^2 cps per ppm per nA) respectively, than that reported by Ottolini *et al.* (~8).[46]

CONCLUSION

We show that the Li and Be contents can be measured with a CAMECA IMS 1280-HR instrument in one sequence with high accuracy and precision. For lithium, the internal precision can be better than 0.42%, and the spot-to-spot reproducibility is better than 2.71%. The external precision of samples with ppm-level lithium can be as good as 1.48%, which is good enough for elemental analysis. For beryllium, the internal precision can be better than 0.93%, and the spot-to-spot reproducibility is better than 4.68% for tens of ppb beryllium. For the Li and Be contents, the difference between the calibrated SIMS elemental contents and the previously reported recommended value is generally below 5.1% and 7.9%, respectively. The LOD of lithium and beryllium is ~0.04 ppb and ~0.01 ppb, respectively. All these demonstrate the reliability of this analytical technique for low-Li-Be samples.

ASSOCIATED CONTENT

Supporting information (Tables S1 and S2) is available at www.at-spectrosc.com/as/home

AUTHOR INFORMATION

Xiao-Ping Xia is a research professor of geochemistry at Hubei Key Laboratory of Petroleum Geochemistry and Environment, College of Resources and Environment, Yangtze University. He received his B.S. degree in Geochemistry from University of Science and Technology of China (USTC) in 2001, and completed Ph.D. in Geochemistry from the University of Hong Kong (HKU) in 2005. He worked as a postdoctoral research fellow and honorary assistant professor from 2005 to 2009 at HKU. His research focused on developing new technology and new methodology for micro-analyses of geochemistry and their applications. He developed a series of new analytical method using LA-ICPMS and SIMS. His newly developed technology and device for high vacuum LG-SIMS analyses firstly lowered the background water of LG-SIMS analyses to about 0.15 ppm in the world. He is also interested to study the evolutions of the Paleotethys Ocean and determined the exact position of the suture and rifting/closing timing of the Ailaoshan Ocean and established a new bipolar subduction model for the ocean evolution. He published over 160 papers in

SCI journals and six of them were selected as journal cover paper.

Corresponding Author

* X. -P. Xia

Email address: xpxia@yangtzeu.edu.cn

Notes

The authors declare no competing financial interest.

ACKNOWLEDGMENTS

This work was jointly supported by the China National Key R & D Program (2018YFA0702600), the Director's Fund of Guangzhou Institute of Geochemistry, CAS (2022SZJJZD-03), the fund of GIGCAS (IS-3485), and the NSFC (42077404 and 42303024).

REFERENCES

1. R. L. Linnen, M. Van Lichtervelde, and P. Cerny, *Elements*, 2012, **8**, 275-280. https://doi.org/10.2113/gselements.8.4.275
2. A. R. Chakhmouradian, M. P. Smith, and J. Kynicky, *Ore Geol. Rev.*, 2015, **64**, 455-458. https://doi.org/10.1016/j.oregeorev.2014.06.008
3. J. Chen, *Sci. Technol. Rev.* (in Chinese), 2019, **37**, 1.
4. Z. Q. Hou, J. Chen, and M. G. Zhai, *Sci. Bull.*, 2020, **65**, 3651-3652. https://doi.org/10.1360/TB-2020-1417
5. C. Li, D. H. Wang, W. J. Qu, M. H. Ming, L. M. Zhou, X. T. Fan, X. W. Li, H. Zhao, H. L. Wen, and P. C. Sun, *Rock Miner. Anal.* 2020, **39**, 658-669. https://www.cgsjournals.com/zgdzdcqkw-data/ykcs/2020/5/PDF/yk201907310115.pdf
6. H. Hu, R. C. Wang, X. D. Che, W. K. Jin, Z. M. Tang, L. Xie, and X. Y. Tao, *Acta Petrol. Sin.*, 2022, **38,** 1890-1900. https://doi.org/10.18654/1000-0569/2022.07.05
7. P. W. Gruber, P. A. Medina, G. A. Keoleian, S. E. Kesler, M. P. Everson, and T. J. Wallington, *J. Ind. Ecol.*, 2011, **15**, 760-775. https://doi.org/10.1111/j.1530-9290.2011.00359.x
8. Y. Y. Gao, X. H. Li, W. L. Griffin, Y. J. Tang, N. J. Pearson, Y. Liu, M. F. Chu, Q. L. Li, G. Q. Tang, and S. Y. O'Reilly, *Sci. Rep.-UK*, 2015, **5**, 16878. https://doi.org/10.1038/srep16878
9. S. E. Kesler, P. W. Gruber, P. A. Medina, G. A. Keoleian, M. P. Everson, and T. J. Wallington, *Ore Geol. Rev.*, 2012, **48**, 55-69. 10.1016/j.oregeorev.2012.05.006
10. J. L. Sullivan and L. Gaines, *Ener. Convers Manage.*, 2012, **58**, 134-148. https://doi.org/10.1016/j.enconman.2012.01.001
11. S. R. Dailey, E. H. Christiansen, M. J. Dorais, B. J. Kowallis, D. P. Fernandez, and D. M. Johnson, *Am. Mineral.*, 2018, **103**, 1228-1252. https://doi.org/10.2138/am-2018-6256
12. M. Tiepolo, A. Zanetti, and R. Vannucci, *Geostand. Geoanal. Res.*, 2005, **29**, 211-224. https://doi.org/10.1111/j.1751-908X.2005.tb00893.x
13. P. Černý, *Geosci. Can.*, 1991, **18**, 49-81. https://journals.lib.unb.ca/index.php/GC/article/view/3722
14. M. D. Barton and S. Young, *Rev. Mineral. Geochem.*, 2002, **50**, 591-691. https://doi.org/10.2138/rmg.2002.50.14
15. R. A. Shaw, K. M. Goodenough, N. M. W. Roberts, M. S. A. Horstwood, S. R. Chenery, and A. G. Gunn, *Precambrian Res.*, 2016, **281**, 338-362. https://doi.org/10.1016/j.precamres.2016.06.008
16. T. R. Benson, M. A. Coble, J. J. Rytuba, and G. A. Mahood, *Nat. Commun.*, 2017, **8**, 270. https://doi.org/10.1038/s41467-017-00234-y
17. D. London and J. M. Evensen, *Rev. Mineral. Geochem.*, 2002, **50**. 445-486. https://doi.org/10.2138/rmg.2002.50.11
18. P. Cerny, D. London, and M. Novak, *Elements*, 2012, **8**, 289-294. https://doi.org/10.2113/gselements.8.4.289
19. D. London and G. B. Morgan, *Elements*, 2012, **8**, 263-268. https://doi.org/10.2113/gselements.8.4.263
20. P. Thomason, *Anal. Chem.*, 1956, **28**, 1527-1530. https://doi.org/10.1021/ac60118a007
21. B. Little, S. Platman, and R. Fieve, *Clin. Chem.*, 1968, **14**, 1211-1217. https://doi.org/10.1093/clinchem/14.12.1211
22. J. Chapman and L. Dale, *Anal. Chim. Acta*, 1976, **87**, 91-95. https://doi.org/10.1016/S0003-2670(01)83123-8
23. K. Nakashima, S. i. Nakatsuji, S. Akiyama, T. Kaneda, and S. Misumi, *Chem. Lett.*, 1982, **11**, 1781-1782. https://doi.org/10.1246/cl.1982.1781
24. K. Hiratani, M. Nomoto, H. Sugihara, and T. Okada, *Chem. Lett.*, 1990, **19**, 43-46. https://doi.org/10.1246/cl.1990.43
25. M. Tabata, J. Nishimoto, and T. Kusano, *Talanta*, 1998, **46**, 703-709. https://doi.org/10.1016/s0039-9140(97)00327-5
26. B. Rumbelow and M. Peake, *Ann. Clin. Biochem.*, 2001, **38**, 684-686. https://doi.org/10.1258/0004563011900894
27. S. Gao, X. M. Liu, H. L. Yuan, B. Hattendorf, D. Gunther, L. Chen, and S. H. Hu, *Geostand.Newsl.*, 2002, **26**, 181-196. https://doi.org/10.1111/j.1751-908X.2002.tb00886.x
28. M. Tiepolo, A. Zanetti, and R. Vannucci, *Geostand. Geoanal. Res.*, 2005, **29**. 211-224. https://doi.org/10.1111/j.1751-908X.2005.tb00893.x
29. D. E. Jacob, *Geostand. Geoanal. Res.*, 2006, **30**, 221-235. https://doi.org/10.1111/j.1751-908X.2006.tb01064.x
30. Y. Xue, S. Bai, and T. L. Deng, *Guangdong Weiliang Yuansu Kexue*, 2006, **13**, 6-10. https://kns.cnki.net/kcms2/article/abstract?v=b4E8SuETvlLe_E42K2FQmjPH30OAnuiGgyDCqYPRn9H1A70M8O811FpSn6HPUnONyCGO3gwPoHpZDxQqhxs1IHkLzKFfS-orhOYsxFRXr8ix_mGFv0cwilVo0BbulOt9DdNtRzv49a2hVKYFN7nM3A==&uniplatform=NZKPT&language=CHS
31. Y. Liu, Z. Hu, S. Gao, D. Günther, J. Xu, C. Gao, and H. Chen, *Chem. Geol.*, 2008, **257**, 34-43. https://doi.org/10.1016/j.chemgeo.2008.08.004
32. A.-S. Bouvier, T. Ushikubo, N. T. Kita, A. J. Cavosie, R. Kozdon, and J. W. Valley, *Contrib. Mineral. Petr.*, 2011, **163**, 745-768. https://doi.org/10.1007/s00410-011-0697-1
33. I. D. Manfro, M. Tegner, M. E. Krutzmann, A. D. C. Artmann, M. R. Brandeburski, G. P. Peteffi, R. Linden, and M. V. Antunes, *Talanta*, 2020, **216**, 120907. https://doi.org/10.1016/j.talanta.2020.120907e
34. K. Mukai, R. Kasada, K. Sasaki, and S. Konishi, *J. Phys. Chem. C*, 2020, **124**, 9256-9260. https://doi.org/10.1021/acs.jpcc.0c02885

35. A. Winckelmann, S. Nowak, S. Richter, S. Recknagel, J. Riedel, J. Vogl, U. Panne, and C. Abad, *Anal. Chem.*, 2021, **93**, 10022-10030. https://doi.org/10.1021/acs.analchem.1c00206
36. T. Schirmer, M. Wahl, W. Bock, and M. Kopnarski, *Metals*, 2021, **11**, 825. https://doi.org/10.3390/met11050825
37. H. Takahashi, T. Murano, M. Takakura, S. Asahina, M. Terauchi, M. Koike, T. Imazono, M. Koeda, and T. Nagano, *IOP Conf. Ser.: Mater. Sci. Eng.*, 2016, **109**, 012017. https://doi.org/10.1088/1757-899x/109/1/012017
38. S. Kimoto, H. Hashimoto, and H. Uchiyama, in *Vth International Congress on X-Ray Optics and Microanalysis / V. Internationaler Kongreß für Röntgenoptik und Mikroanalyse / Ve Congrès International sur l'Optique des Rayons X et la Microanalyse*, ed. G. Möllenstedt, K. H. Gaukler. Springer Berlin Heidelberg: Berlin, Heidelberg, 1969, pp 369-372.
39. M. D. Dyar, M. Wiedenbeck, D. Robertson, L. R. Cross, J. S. Delaney, K. Ferguson, C. A. Francis, E. S. Grew, C. V. Guidotti, R. L. Hervig, J. M. Hughes, J. Husler, W. Leeman, A. V. McGuire, D. Rhede, H. Rothe, R. L. Paul, I. Richards, and M. Yates, *Geostand. Geoanal. Res.*, 2001, **25**, 441-463. https://doi.org/10.1111/j.1751-908X.2001.tb00616.x
40. H. R. Marschall and T. Ludwig, *Miner. Petrol.*, 2004, **81**, 265-278. https://doi.org/10.1007/s00710-004-0037-5
41. K. P. Jochum, B. Stoll, K. Herwig, M. Willbold, A. W. Hofmann, M. Amini, S. Aarburg, W. Abouchami, E. Hellebrand, B. Mocek, I. Raczek, A. Stracke, O. Alard, C. Bouman, S. Becker, M. Dücking, H. Brätz, R. Klemd, D. de Bruin, D. Canil, D. Cornell, C.-J. de Hoog, C. Dalpé, L. Danyushevsky, A. Eisenhauer, Y. Gao, J. E. Snow, N. Groschopf, D. Günther, C. Latkoczy, M. Guillong, E. H. Hauri, H. E. Höfer, Y. Lahaye, K. Horz, D. E. Jacob, S. A. Kasemann, A. J. R. Kent, T. Ludwig, T. Zack, P. R. D. Mason, A. Meixner, M. Rosner, K. Misawa, B. P. Nash, J. Pfänder, W. R. Premo, W. D. Sun, M. Tiepolo, R. Vannucci, T. Vennemann, D. Wayne, and J. D. Woodhead, *Geochem. Geophy. Geosy.*, 2006, **7**, 1-44. https://doi.org/10.1029/2005gc001060
42. M. C. Jollands, A. D. Burnham, H. S. C. O'Neill, J. Hermann, and Q. Qian, *Earth Planet. Sc. Lett.*, 2016, **450**, 71-82. https://doi.org/10.1016/j.epsl.2016.06.028
43. V. V. Khiller, *News of the Ural State Mining University*, 2017, 52-56. https://doi.org/10.21440/2307-2091-2017-4-52-56
44. R. Rybka and R. Wolf, in *X-ray spectrometry in electron beam instruments.* Springer, 1995, pp 287-303. https://link.springer.com/book/10.1007/978-1-4615-1825-9
45. W. Zhang, X. Che, R. Wang, L. Xie, X. Li, and D. Zhang, *Sci. Bull.*, 2020, **65**, 3205-3216. https://doi.org/10.1360/TB-2020-0316
46. L. Ottolini, P. Bottazzi, and R. Vannucci, *Anal. Chem.*, 1993, **65**, 1960-1968. https://doi.org/10.1021/ac00063a007
47. J. Cabato, R. Altherr, T. Ludwig, and H.-P. Meyer, *Contrib. Mineral. Petr.*, 2013, **165**, 1135-1154. https://doi.org/10.1007/s00410-013-0851-z
48. Y. Lahaye, D. Lambert, and S. Walters, *Geostand.Newsl.*, 1997, **21**, 205-214. https://doi.org/10.1111/j.1751-908X.1997.tb00671.x
49. A. Rocholl, *Geostand. Geoanal. Res.*, 1998, **22**, 33-45. https://doi.org/10.1111/j.1751-908X.1998.tb00543.x
50. A. J. R. Kent, B. Jacobsen, D. W. Peate, T. E. Waight, and J. A. Baker, *Geostand. Geoanal. Res.*, 2004, **28**, 417-429. https://doi.org/10.1111/j.1751-908X.2004.tb00760.x
51. L. Strnad, M. Mihaljevic, and O. Sebek, *Geostand. Geoanal. Res.*, 2005, **29**, 303-314. https://doi.org/10.1111/j.1751-908X.2005.tb00902.x
52. K. P. Jochum, L. Nohl, K. Herwig, E. Lammel, B. Stoll, and A. W. Hofmann, *Geostand. Geoanal. Res.*, 2005, **29**, 333-338. https://doi.org/10.1111/j.1751-908X.2005.tb00904.x
53. K. P. Jochum, M. Willbold, I. Raczek, B. Stoll, and K. Herwig, *Geostand. Geoanal. Res.*, 2005, **29**, 285-302. https://doi.org/10.1111/j.1751-908X.2005.tb00901.x
54. Z. Hu, Y. Liu, M. Li, S. Gao, and L. Zhao, *Geostand. Geoanal. Res.*, 2009, **33**, 319-335. https://doi.org/10.1111/j.1751-908X.2009.00030.x
55. K. P. Jochum, B. Stoll, K. Herwig, and M. Willbold, *J. Anal. At. Spectrom.*, 2007, **22**, 112-121. https://doi.org/10.1039/b609547j
56. R. B. Ickert and R. A. Stern, *Geostand. Geoanal. Res.*, 2013, **37**, 429-448. https://doi.org/10.1111/j.1751-908X.2013.00222.x
57. X. P. Xia, Z. X. Cui, W. C. Li, W. F. Zhang, Q. Yang, H. J. Hui, and C. K. Lai, *J. Anal. At. Spectrom.*, 2019, **34**, 1088-1097. https://doi.org/10.1039/c9ja00073a
58. Z. Cui, Q. Yang, X.-P. Xia, R. Wang, M. Bonifacie, C.-K. Lai, W.-F. Zhang, Y.-Q. Zhang, and J. Xu, *J. Anal. At. Spectrom.*, 2022, **37**, 222-228. https://doi.org/10.1039/d1ja00347j
59. Z. X. Cui, X. P. Xia, Q. Yang, B. Gong, W. F. Zhang, Y. Q. Zhang, and C. K. Lai, *Atom. Spectrosc.*, 2022, **43**, 70-76. https://doi.org/10.46770/AS.2022.006
60. G.-Q. Tang, X.-H. Li, Q.-L. Li, Y. Liu, X.-X. Ling, and Q.-Z. Yin, *J. Anal. At. Spectrom.*, 2015, **30**, 950-956. https://doi.org/10.1039/C4JA00458B
61. J. L. Mosenfelder, M. Le Voyer, G. R. Rossman, Y. Guan, D. R. Bell, P. D. Asimow, and J. M. Eiler, *Am. Mineral.*, 2011, **96**, 1725-1741. https://doi.org/10.2138/am.2011.3810
62. M. Le Voyer, P. D. Asimow, J. L. Mosenfelder, Y. Guan, P. J. Wallace, P. Schiano, E. M. Stolper, and J. M. Eiler, *J. Petrol.*, 2014, **55**, 685-707. https://doi.org/10.1093/petrology/egu003